

## Experiments with Turbulent Soap Films

H. Kellay,\* X.-I. Wu, and W. I. Goldburg

*Department of Physics and Astronomy, University of Pittsburgh, Pittsburgh, Pennsylvania 15260*

(Received 17 November 1994)

A vertical soap film channel driven by gravity is used to study two-dimensional turbulence. Velocity differences on different scales and the spectrum of velocity fluctuations show behavior very different from their three-dimensional counterparts. Our findings are consistent with the theoretically predicted enstrophy cascade picture for two-dimensional turbulence. However, significant differences were observed.

PACS numbers: 47.27.Gs, 68.15.+e

Many theoretical studies and the few experiments that exist leave little doubt that two-dimensional (2D) turbulence and three-dimensional turbulence are very different. One might expect that numerical studies, being so much easier in two dimensions rather than three, might have resolved all the fundamental issues at stake, but this is not the case.

Herein we describe a study of a soap film [1] that flows between two parallel vertical wires. Though there probably is appreciable damping of the flow by the coupling between the moving film and the air surrounding it, the velocity field in the film exhibits features that one associates with 2D turbulent flow. In spite of this coupling, a soap film is sufficiently thin (thickness typically several  $\mu\text{m}$ ) that the direction of the vorticity  $\omega$  is almost fully perpendicular to the plane of the film. Components of  $\omega$  in the plane of the film are very heavily damped.

Because  $\omega$  is perpendicular to the flow field  $\mathbf{v}$ , an important turbulence-generating mechanism is absent, namely vortex stretching [2]. Another distinguishing feature of 2D turbulence is the appearance of a second conserved quantity in the absence of dissipation, namely the mean-square vorticity, also called the enstrophy. In the 2D case, Kolmogorov-like arguments and detailed calculations suggest that for scales  $\ell$  greater than the injection scale  $\ell_{\text{inj}}$ , there is an energy cascade to eddies of larger size. For  $\ell < \ell_{\text{inj}}$  there is an enstrophy cascade to smaller eddies [3,4]. For the energy cascade, it is believed that the mean difference in velocity between two points separated by a distance  $\ell$  scales as  $\langle \delta v(\ell) \rangle \propto \ell^\alpha$  with  $\alpha = 1/3$ , as in the 3D case. On the other hand, for the enstrophy cascade the same sort of scaling arguments yield  $\alpha = 1$ . These predictions are applicable only to homogeneous and isotropic turbulence.

We have probed turbulence in the soap film by two methods. One of them, homodyne photon correlation spectroscopy (HCS) [5], has the advantage of not requiring the employment of Taylor frozen turbulence hypothesis. According to this hypothesis, the structure of the small eddies does not change as they are swept across the observation point by the mean flow. The method per-

mits one to explore a selected component of the velocity difference  $\delta \mathbf{v}(\ell) = \mathbf{v}(\mathbf{r} + \ell) - \mathbf{v}(\mathbf{r})$  on a scale  $\ell$ . More precisely, the HCS scheme yields the cosine transform of the probability density function  $P(\delta v(\ell))$ , that is its symmetric part, and the width  $\bar{\delta v}(\ell)$  of  $P$ . Here  $v$  is the component of  $\mathbf{v}$  along the momentum transfer vector  $\mathbf{q}$ , as discussed below. A disadvantage of the HCS scheme, as we have used it, is that  $\ell$  is limited to several millimeters for photon coherence reasons [6]. In the present experiments  $\ell$  was varied from 0.06 to 0.4 cm.

We also measured the power spectrum of the velocity fluctuations  $S_{xx}(f) = \langle v_x(f)v_x^*(f) \rangle$  and  $S_{yy}(f) = \langle v_y(f)v_y^*(f) \rangle$ . Here  $v_x(t)$  and  $v_y(t)$  are, respectively, velocity fluctuations perpendicular to the flow direction and parallel to it, and  $f$  is the frequency. The brackets designate time or ensemble averages. These spectral measurements are made at a fixed point in the film, and the Taylor frozen turbulence assumption is used to relate the temporal measurements to spatial ones, i.e.,  $f = k_y V / 2\pi = V / \ell$ , where  $V$  is the mean flow velocity (which is in the  $y$  direction) and  $\mathbf{k}$  is the wave vector. These spectral measurements were made with a novel fiber velocimeter to be described below. The experiment explored velocity fluctuations on large scales  $\ell = 2\pi/k_y$  between 0.2 and 20 cm. If the turbulence is isotropic  $S_{xx} = S_{yy}$ , a condition that could be achieved,  $S_{xx}$  and  $S_{yy}$  are related to the energy spectrum of the turbulence,  $E(k)$ . At large  $f$  (small  $\ell$ ) the velocimeter measurements and the HCS measurements of  $\bar{\delta v}(\ell)$  are in agreement with each other. They are also reasonably consistent with calculations [3] and observations [7] that indicate that the mean-square vorticity, or enstrophy, cascades from larger eddies to smaller ones.

The soap film channel was driven by gravity and fed by a reservoir which was filled with soapy water. The film spanned a pair of parallel vertical wires of separation  $W = 5$  cm that were attached to the reservoir floor. The soap solution in the reservoir was fed into the film by small holes, of radius  $R = 0.02$  cm, drilled into the reservoir bottom. The wires were weighted at the bottom end, and these weights were suspended in a second reservoir also filled with soapy water. The length

of the wires was 180 cm. The soap solution consisted of a commercial detergent of concentration 4% and glycerol of concentration 5% in distilled water. The glycerol increases the lifetime of the film, which could flow for many hours without breaking.

The level  $H$  of soap solution in the upper reservoir controlled the mean vertical film speed  $V$ . To a good approximation, it was found that  $V = n\pi R^2 \sqrt{2gH}/W\bar{h}$ , where  $n$  is the number of holes,  $g$  is the gravitational constant, and  $\bar{h}$  is the mean thickness of the film. For  $\bar{h} \approx 5 \mu\text{m}$ ,  $V$  could be varied between 20 cm/s and about 4 m/s. We could not study the small-velocity, laminar flow regime in this channel, as a convective instability sets in, producing backflow of patches of thin film. The velocity  $V$  was measured using laser Doppler velocimetry (LDV). From a measurement of  $V$  and the total fluid flux (in  $\text{cm}^3/\text{s}$ ), one obtains an estimate of the mean film thickness  $\bar{h}$ , which was typically  $5 \mu\text{m}$ .

Because the HCS scheme is not widely used, it is necessary to describe it briefly before turning to the experimental results themselves. As in LDV, one seeds the fluid with small particles which scatter the light. The seed particles were polystyrene spheres having a diameter of  $0.1 \mu\text{m}$ . The light source was a 300 mW argon laser beam of vacuum wavelength  $\lambda = 514 \text{ nm}$ . A prism splits the beam into two mildly focused beams brought with two mirrors to form two horizontally oriented bright spots of adjustable spacing  $\ell$  on the flowing film.

The incident beams were at  $45^\circ$  with respect to the film. The scattered light was recorded by a photomultiplier located on the opposite side of the film at a scattering angle  $\theta$  of  $90^\circ$ . The scattering plane was horizontal, assuring that the scattering vector  $\mathbf{q}$  was perpendicular to the flow direction. The magnitude of the scattering vector  $\mathbf{q}$  is given by  $q = (4\pi n/\lambda) \sin(\theta/2)$ , where  $n (= 1.33)$  is the refractive index of the film. With the above geometry, the measurements are insensitive to velocity variations in the flow direction.

The scattered light intensity  $I(t)$  reaching the photomultiplier is sent to a digital correlator, which records the auto-correlation function  $g(t) = \langle I(t')I(t' + t) \rangle / \langle I(t') \rangle^2$ , where the brackets indicate an average over  $t'$ . This function consists of an uninteresting time-independent part and a time varying part  $G(t)$ , which within a multiplicative constant is the cosine transform of  $P(\delta v(\ell))$ , i.e.,

$$G(t) = \int P(\delta v(\ell)) \cos[q\delta v(\ell)t] d\delta v(\ell). \quad (1)$$

If  $P$  has the self-similar form  $P(\delta v(\ell)) = \delta v(\ell)^{-1} Q(\delta v(\ell)/\delta v(\ell))$  and if  $\delta v(\ell) \propto \ell^\alpha$ , then  $G(t)$  will also be self-similar, i.e.,  $G(t) = G(q\delta v(\ell)t) = G(q\ell^\alpha t)$ . The exponent  $\alpha$  is determined by plotting a series of curves  $G(t)$  vs  $t\ell^\alpha$  for a range of  $\ell$  and varying  $\alpha$  to bring them into superposition. For this experiment we identify the width of  $P(\delta v(\ell))$  with the  $1/e$  time of  $G(t)$  and note it as  $\langle \delta v(\ell) \rangle$ .

The HCS measurements were carried out at a distance of 80 cm from the entrance of the channel and for a mean flow speed  $V$  of roughly 1 m/s. A comb (i.e., a one-dimensional grid) was inserted into the film, and the velocity field was probed at distances  $Y = 0.5$  and 2.7 cm below this comb and at a point equally distant from the parallel wires. The teeth spacing of the comb was  $M = 0.1 \text{ cm}$ .

Figure 1 shows the extent to which  $G(t)$  [and hence  $P(\delta v(\ell))$ ] has the simple scaling form discussed below Eq. (1). A set of measurements were made at four values of  $\ell$ , as designated in the figure caption. The measured  $G(t)$  was rescaled by multiplying the time variable by  $\ell^\alpha$  to see if they could be superimposed. We show the results for three values of  $\alpha$  so one can see that the preferred choice is  $\alpha = 1$  with an uncertainty that we estimate as  $\pm 0.5$ . There is simply no self-similarity if one uses the 3D exponent  $\alpha = 1/3$ . As already noted, an  $\alpha$  value of unity corresponds to an enstrophy cascade from large to small scales. The functional form of  $G(t)$  is closer to being a Lorentzian, implying that  $P$  is a decaying exponential function. This finding for the soap film is in contrast with measurements in 3D flows in water tunnels where  $G(t)$  decays exponentially [5,8].

Figure 2 is a plot of  $\tau^{-1}(\ell) = q\langle \delta v(\ell) \rangle$  as a function of  $\ell$  as measured at distances  $Y = 0.5 \text{ cm}$  (curve *a*) and 2.7 cm (curve *b*) below the comb. A typical relaxation time  $\tau$  of  $G(t)$  for  $\ell \sim 0.2 \text{ cm}$  is approximately  $3 \mu\text{s}$ , which corresponds to a characteristic velocity  $\langle \delta v \rangle = 1/q\tau \approx 1.5 \text{ cm/s}$ . Here, a linear increase of  $\langle \delta v \rangle$  with  $\ell$  is again observed, except when  $\ell < 0.15 \text{ cm}$ , where  $\langle \delta v(\ell) \rangle$  loses its  $\ell$  dependence. This effect arises from the fact that

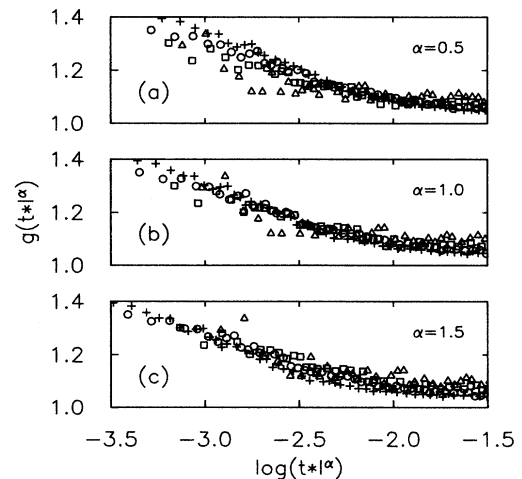


FIG. 1. Scaling form of the intensity-intensity autocorrelation function. The data have been rescaled to  $t\ell^\alpha$  with  $\alpha = 0.5$  (a), 1.0 (b), and 1.5 (c). The scattering volume was at  $Y = 0.5 \text{ cm}$  below the comb with  $M = 0.1 \text{ cm}$ , and the mean flow velocity was 1 m/s. Here  $\ell$  is 0.4 cm (triangles), 0.29 cm (squares), 0.19 cm (circles), and 0.14 cm (crosses).

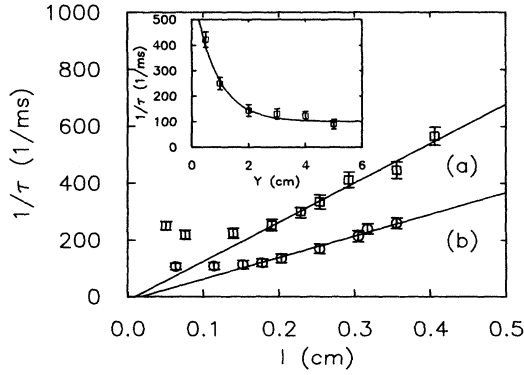


FIG. 2. Inverse decay time  $1/\tau$  as a function of length scale  $\ell$ . Curves *a* and *b* are for scattering volume at  $Y = 0.5$  and  $2.7$  cm below the grid, respectively. The mean velocity of the flow is  $1$  m/s. Inset:  $1/\tau$  for fixed  $\ell = 0.28$  cm and for different distances from the comb with  $M = 0.1$  cm.

the two beams passing through the film are not parallel and therefore correspond to different values of  $q$ . This introduces an  $\ell$ -independent term in  $G(t)$  of the form  $\Delta \mathbf{q} \cdot \mathbf{V}$  that dominates the decay of  $G(t)$  when  $\ell < 0.15$  cm.

It is apparent from a comparison of *a* and *b* in Fig. 2 that the slope of  $\langle \delta v(\ell) \rangle$  vs  $\ell$  is much larger at the observation point  $Y = 0.5$  cm than at the more distant point  $Y = 2.7$  cm. Thus the amplitude of the velocity fluctuations decreases with increasing  $Y$ . This finding is more clearly seen in the inset of this figure, which shows  $\langle \delta v \rangle$  vs  $Y$  for a fixed  $\ell = 0.28$  cm. Other measurements, made very far below the comb ( $Y > 10$  cm) establish that  $\langle \delta v(\ell) \rangle$  ceases to decrease with increasing  $Y$ , as the flow loses memory of the presence of the comb.

Our finding,  $\alpha \approx 1$ , is consistent with the flow in the soap film being laminar as well as being consistent with an enstrophy cascade. If the flow were laminar,  $\alpha$  would be unity if  $\langle \delta v(\ell) \rangle$  were measured in the direction of the flow. However, the HCS measurements were made in the transverse direction such that  $\mathbf{q} \cdot \mathbf{V} = 0$ . Laminar flow would produce no velocity differences with this geometry and  $G(t)$  will decay only by virtue of Brownian motion of the seed particles. Additional evidence that the flow is not laminar comes from data taken with the vibrating fiber velocimeter.

The velocimeter consists of an optical fiber connected to the output of a small laser. The fiber penetrates the film (without rupturing it), and its deflection  $x(t)$  and  $y(t)$  were separately recorded. The fiber penetrated less than  $1$  mm through the film, and the deflection of this glowing end was measured with a position-sensitive detector. The fiber was clamped at a point  $L$  a few millimeters from the film. This very short fiber length allows for a relatively high resonance frequency  $f_0 = 2.5$  kHz. Useful measurements of  $S_{xx}(f)$  and  $S_{yy}(f)$  can be made at  $f$  appreciably less than  $f_0$ . The chosen value of  $f_0$  was a reasonable compromise that gave an adequate signal-to-

noise ratio. Separate calibration runs established that the fiber deflection is proportional to the velocity. The fiber perturbs the fluid motion but only for a radial distance comparable to its diameter, which is  $50 \mu\text{m}$ .

The output of the position-sensitive detector is fed to a spectrum analyzer (HP 3561A), which displays the power spectrum of  $S_{xx}(f)$  and  $S_{yy}(f)$  of the velocity fluctuations  $v_x(t)$  and  $v_y(t)$ . Invoking the Taylor hypothesis, one can calculate one-dimensional (1D) spectra  $S_{yy}(k_y) = S_{yy}(2\pi f/V)$  and  $S_{xx}(k_x) = S_{xx}(2\pi f/V)$ . If the turbulence is isotropic and homogeneous, and if the 1D spectra  $S_{yy}(k_y)$  and  $S_{xx}(k_x)$  show power-law behavior, the spectra would have the same power-law dependence as  $E(k)$  [9]. Typically,  $V = 2$  m/s, so that the largest  $k$  or the smallest length scale that could be probed by the velocimeter was  $\ell = V/f \approx 0.2$  cm.

To produce nearly isotropic turbulence  $S_{xx}(f) \approx S_{yy}(f)$ , a comb was inserted through the film. For a few centimeters below it these two spectra were roughly equal, implying that the turbulence is isotropic. In Fig. 3, the lower two spectra are for transverse and longitudinal velocity fluctuations taken at  $4$  cm from a comb with  $M = 0.3$  cm. In this log-log plot  $S_{xx}(f)$  and  $S_{yy}(f)$  appear to be roughly the same for most of the frequency range covered. One sees that these spectra could be described as being of algebraic form,  $S_{yy}(f) \sim f^{-\mu}$  for most of the frequency range, while  $S_{xx}(f) \sim f^{-\mu}$  only for the high-frequency range  $100 < f < 1000$  Hz. The limiting slope here is roughly  $\mu \sim 3.3$ .

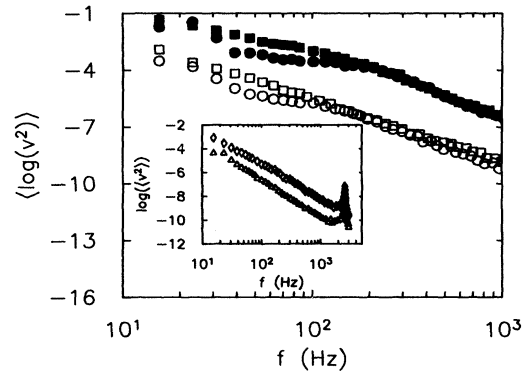


FIG. 3. Power spectrum of the fiber position fluctuations or equivalently the velocity fluctuations measured at a distance of  $80$  cm from the entrance of the channel. The lower two spectra are for the longitudinal  $S_{yy}(f)$  (open squares) and transverse  $S_{xx}(f)$  (open circles) velocity fluctuations at  $4$  cm behind a comb with  $M = 0.3$  cm. The upper two spectra are for longitudinal (filled squares) and transverse (filled circles) fluctuations as measured at  $1$  cm behind a comb with  $M = 0.1$  cm. Inset: spectra in the absence of the comb as measured at a distance of  $80$  cm from the entrance of the channel. The diamonds are for longitudinal fluctuations, and the triangles are for transverse ones. Here  $V = 2$  m/s. In this inset we display the power spectra out to  $f = 10^4$  Hz, so that the effect of the resonant frequency of the fiber may be seen.

Measurements were also carried out for a smaller teeth spacing  $M$  and close to the comb. The functional shape of the spectra changes measurably when  $M$  is changed. The two upper spectra in Fig. 3 are taken at 1 cm behind a comb with  $M = 0.1$  cm. Here the spectra could be described as being of algebraic form only at the high-frequency range  $100 < f < 1000$  Hz. The slope for this range is about 3.6, whereas the HCS measurements of  $\alpha$  imply a  $\mu = 2\alpha + 1 \approx 3$ . At the low-frequency end of the spectrum,  $10 < f < 200$  Hz, the slope  $\mu$  is approximately 2 for the longitudinal component and much less for the transverse one, though the data do not span a wide enough frequency range to permit assigning a meaningful value to this exponent. If this decrease in slope were indicative of a crossover to an inverse energy cascade [3], this slope would presumably be  $5/3$ . Gharib and Derango [7] have used LDV to study turbulence behind a grid in a soap film, and their results are consistent with an inverse energy cascade ( $\mu = 5/3$ ) and a direct enstrophy cascade ( $\mu = 3$ ). They were able to explore roughly a third of a decade of the inverse energy cascade, and hence these inverse cascade measurements cannot be regarded as conclusive.

In our experiment the decrease in slope at small  $f$  (or large scales) in Fig. 3 may have a different origin. The inset of Fig. 2 shows that the turbulence changes as the distance to the comb increases. Thus the change in slope at small  $f$  may arise because the turbulence ceases to be homogeneous in the  $y$  direction when  $f < 100$  Hz, or equivalently when  $\ell$  is greater than 2 cm.

When the comb is removed the energy spectrum is no longer isotropic, with  $S_{yy}(f)/S_{xx}(f) \approx 10$ . On the other hand, the slope  $\mu$  is constant in a log-log plot over a much wider frequency range than when the comb is present. This may be seen in the inset of Fig. 3, where the data show  $S_{yy}$  and  $S_{xx}$  vs  $f$  having a slope that is constant over the frequency interval  $20 < f < 1000$  Hz. The value of  $\mu$  here is roughly 3. Perhaps one sees power-law behavior over a wider frequency range in the comb-free case because the turbulence is then more homogeneous in the  $y$  direction. Note that when  $S_{xx}$  and  $S_{yy}$  are no longer equal,

there is no unambiguous way to relate these spectra to the energy spectrum  $E(k)$ .

In summary, we have measured velocity differences over varying length scales  $\ell$ , using a method (HCS) that does not require invoking the Taylor frozen turbulence assumption. We find that  $\langle \delta v(\ell) \rangle \propto \ell^\alpha$  with  $\alpha$  close to 1 over the interval  $0.1 < \ell < 0.4$  cm. The technique, which measures the cosine transform of the probability density for such velocity differences, shows that  $P(\delta v(\ell))$  is self-similar and of exponential form in the millimeter to submillimeter range of  $\ell$ . Generally the HCS results were corroborated by the spectral measurements made with a fiber velocimeter which probes length scales from  $\ell = 0.2$  to 20 cm. Both sets of measurements are consistent with the appearance of the enstrophy cascade towards small scales as expected for 2D turbulence.

We have profited from discussions with B. Martin, C. Cheung, C.H. van Atta, D. Lohse, and D. Jasnow. This research was supported by the National Science Foundation, Grant No. DMR-8914351.

---

\*Present address: CPMOH, Universite de Bordeaux I, 351 Cours de la Liberation, 33405 Talence Cedex, France.

- [1] Y. Couder, J. Phys. (Paris), Lett. **45**, L-353 (1984); Y. Couder, J.M. Chomaz, and M. Rabaud, Physica (Amsterdam) **37D**, 384 (1989).
- [2] D.J. Tritton, *Physical Fluid Dynamics* (Oxford Science Publications, Oxford, 1988), 2nd ed.
- [3] R.H. Kraichnan, Phys. Fluids **10**, 1417 (1967).
- [4] M. Lesieur, *Turbulence in Fluids* (Kluwer Academic Publ., Dordrecht, 1990), 2nd ed.
- [5] P. Tong, W.I. Goldburg, C.K. Chan, and A. Sirivat, Phys. Rev. A **37**, 2125 (1988).
- [6] K.J. Maloy, W.I. Goldburg, and H.K. Pak, Phys. Rev. A **46**, 3288 (1992).
- [7] M. Gharib and P. Derango, Physica (Amsterdam) **37D**, 406 (1989).
- [8] H.K. Pak, W.I. Goldburg, and A. Sirivat, Phys. Rev. Lett. **68**, 938 (1992).
- [9] J.O. Hinze, *Turbulence*, McGraw-Hill Series in Mechanical Engineering (McGraw-Hill, New York, 1975), 2nd ed.